Fast Frequency-Hopping Dynamic Multiple-Access for Cognitive Radios: Noncoherent Interference Cancellation

Shuo Zhang #1, Lie-Liang Yang *2, Youguang Zhang #3

School of Electronic and Information Engineering
Beihang University, Beijing 100191, China
1 sz09v@ecs.soton.ac.uk, 3 zhangyouguang@vip.sina.com

* School of Electonics and Computer Science
University of Southampton, SO17 1BJ, United Kingdom
2 lly@ecs.soton.ac.uk

***Abstract*—This paper proposes a fast frequency-hopping M-ary frequency-shift keying dynamic multiple-access (FFH/MFSK DMA) scheme for application in cognitive radios (CRs). For characterising the performance of the FFH/MFSK DMA systems, primary users (PUs) are assumed to become active according to a Poisson process. In our FFH/MFSK DMA system, the noncoherent majority vote assisted single-user detector (MV-SUD) or noncoherent iterative interference cancellation assisted multiuser detector (IIC-MUD) is employed, in order to implement low-complexity detection. The bit error rate (BER) and throughput performance of the FFH/MFSK DMA systems are investigated, when assuming communications over Nakagami-m fading channels. Our studies show that the FFH/MFSK DMA is a high-flexibility scheme for application in CRs. It is capable of attaining a substantial throughput without degrading the quality-of-service (QoS) of primary radios (PRs).**

I. Introduction

Recently, the studies demonstrate that the radio spectrums regulated by governments and limited only for licensed users are low efficiency in use [3]. The practical measurement shows that most of the licensed spectrum is underutilised. According to the Federal Communications Commission (FCC) [1, 2], for example, temporal and geographical variations in the utilisation of the allocated spectrums range from 15% to 85%. Therefore, for the future generations of wireless communications systems supporting high-speed multimedia services, it is very important to establish high-flexibility and high-reliability access models, which can substantially improve the utilisation efficiency of the valuable spectrums. This motivation has led to the concept of CRs [3], which increase the efficiency of using the radio spectrum resources through introducing opportunistic access of the licensed frequency bands that are underutilised [2–4]. According to [4], in CRs, there are four main functions, including (1) the spectrum sensing for determining available spectrum holes [5] for CR users (CRUs) and detecting the presence of PUs, (2) the spectrum management motivating to make the spectrum-efficiency as high as possible, (3) the spectrum sharing for coordinating the CRUs to access available spectrum and, (4) the spectrum mobility, which copes with seamless transition from one spectrum to another.

This paper addresses the issue of spectrum sharing in CRs, proposes and studies the FFH/MFSK DMA scheme with noncoherent detection [12, 14]. In order to investigate the performance of the FFH/MFSK DMA systems, we assume that the PUs and CRUs are operated in the interweave paradigm [10], where the CRUs can only communicate opportunistically on the frequency bands not occupied by the PUs, and must stop communication, once PUs appear on these bands. We assume that the whole frequency spectrum accessible by the CRUs is divided into a number of frequency bands. Once a PU becomes active, it occupies one to several frequency bands. We assume that PUs activate according to a Poisson process and the duration of activation of a PU obeys exponential distribution. Therefore, the frequency bands possible for the CR system are dynamic and are shared by a number of CRUs. The CRUs access the frequency bands using the FFH/MFSK DMA, which varies the set of FFH frequencies according to the frequency bands available. In this paper, MV-SUD and IIC-MUD are introduced for noncoherent detection of the FFH/MFSK DMA signals. Both BER and throughput performance are investigated, when assuming communication over Nakagami-m fading channels [12]. Our studies show that the FFH/MFSK DMA constitutes one of the promising alternatives for DMA in CRs. It uses noncoherent detection without requiring channel estimation. It has linear complexity and reasonable error and throughput performance owing to making efficient use of the embedded frequency-selective diversity. Furthermore, with the aid of the FFH techniques, it is convenient to implement seamless spectrum transition.

Note that, since the proposal of CRs, DMA has attracted a lot of attention in research, as evidenced by, e.g., [4, 6–8] and the references therein. However, the DMA schemes considered so far for CRs use mainly coherent detection depending on ideal channel state information (CSI), which is hard to acquire in dynamic CR environments. Furthermore, the need of real-time CSI requires extra bandwidth for channel estimation, which unavoidably decreases the CRs' spectrum-efficiency.

II. System Modelling

The spectrum bands considered host two types of users, PUs and CRUs, without cooperation between them. The PUs are the licensed users to use the spectrums, while the CRUs are secondary users that are not pre-assigned spectrums. In this paper, we assume that the PUs and CRUs are operated under the interweave paradigm [10]. Under this paradigm, the CRUs can only communicate opportunistically on the unused spectrums, which are referred to as 'spectrum holes', without affecting the PUs' communication and reducing their QoS. The

CRUs occupying a frequency band must stop communication, once there are PUs presenting.

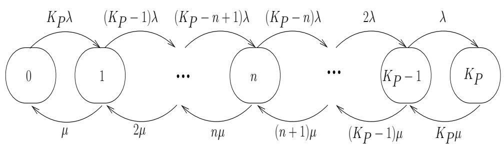

Fig. 1. State transition diagram for modelling the arrival process of PUs.

For the sake of carrying out the related investigation, we assume that the total spectrum accessible by the CRUs consists of C channels, each of which has a fixed and equal bandwidth that is enough for accommodating a MFSK tone. It is assumed that the C channels are allocated to support K_P PUs, which are activated according to the $M/M/K_P/K_P/K_P$ queueing model [9], as depicted in Fig. 1. According to the $M/M/K_P/K_P/K_P$ queueing model, the number of active PUs follows the Poisson distribution associated with a parameter λ representing the arrival rate, the service time obeys the negative exponential distribution with an average service time of $1/\mu$, and the number of parallel service windows, system capacity as well as the total number of customers are the same value of K_P [9, 11]. Furthermore, we assume that $\sum_{k=1}^{K_P} c_k \leq C$, where c_k denotes the number of channels occupied by the kth PU when it communicates.

According to the queueing theory [11], after the system converges to its steady state, the probability that there are n active PUs is

$$P_n = \begin{cases} \dfrac{1}{K_P! \sum_{i=0}^{K_P} \frac{1}{(K_P-i)!i!}\left(\frac{\lambda}{\mu}\right)^i}, & n=0 \\ \dfrac{K_P!}{(K_P-n)!n!}\left(\dfrac{\lambda}{\mu}\right)^n P_0, & 1 \leq n \leq K_P \end{cases} \quad (1)$$

Furthermore, the number of frequency bands available for the CRUs is given by

$$\bar{C} = C - \sum_{k=1}^{K_P} \eta(k) c_k \quad (2)$$

where $\eta(k)$ is a function defined as

$$\eta(k) = \begin{cases} 1, & \text{when the } k\text{th PU is ON} \\ 0, & \text{when the } k\text{th PU is OFF} \end{cases} \quad (3)$$

In this paper, we assume that the channels allocated to an active PU are uniformly and randomly chosen from the unused channels. In this case, the channels available for the CRUs also constitute a Poisson process with its parameters that can be readily derived from the corresponding PUs' Poisson process. For the sake of simplicity, we assume in this paper that $C_P = c_1 = c_2 = \ldots = c_{K_P}$. Then, when there are n active PUs, the number of channels available for the CRUs is

$$\bar{C} = C - nC_P, \ n = 0, 1, \ldots, K_P \quad (4)$$

For the CRUs, we assume that they have the same priority to communicate on the $\bar{C}$ bands, based on a noncoherent FFH/MFSK DMA scheme as considered in the next section.

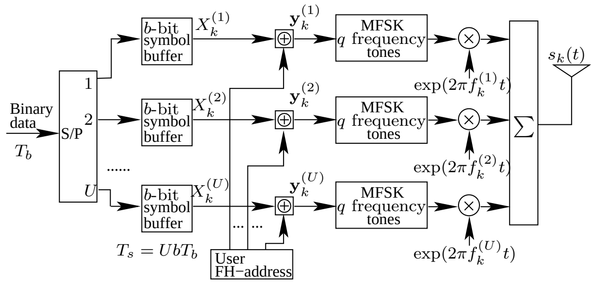

Fig. 2. Transmitter schematic block diagram of the kth CRU in the FFH/MFSK DMA system.

III. FFH/MFSK DMA System

A. Transmitter

The general transmitter schematic block diagram for the kth CRU is shown in Fig. 2. It consists of U sub-streams for the purpose of providing various data rates, each sub-stream carries out both FFH and MFSK operations. As shown in Fig. 2, the input binary bits having a period T_b and a rate R_b is first serial-to-parallel (S/P) converted to U parallel sub-streams. During a MFSK symbol interval of T_s seconds, each sub-stream transmits $b = \log_2 M$ bits representing a MFSK symbol. Hence, we have $T_s = UbT_b$. In order to implement the FFH, the symbol duration T_s is divided into $L = T_s/T_h$ number of time-slots of duration T_h, which is referred to as the FH dwell time. For each of the sub-streams, a frequency is activated from a set of q ($q \geq M$) frequencies, which is determined by the FH address assigned to the kth CRU and the MFSK symbol to be transmitted by the kth CRU. The frequency hops from one to another per T_h seconds.

According to the above description as well as Fig. 2, we can know that the total number of frequency bands required by the general FFH/MFSK DMA system is $Q = Uq$. However, in our forthcoming discourse, we assume for simplicity that $U = 1$ and, hence, $Q = q$. Note that, this simplification does not loss any generality, if we assume that the U sub-streams are operated on U orthogonal frequency bands.

Let the FH address of CRU k be expressed by $\boldsymbol{a}_k = [a_k(0), a_k(1), ..., a_k(L-1)]$ and X_k be the value of the symbol to be transmitted by CRU k. Then, as shown in Fig. 2, X_k is first signatured by $\boldsymbol{a}_k$ as

$$\boldsymbol{y}_k = [y_k(0), y_k(1), ..., y_k(L-1)] = X_k \cdot \mathbf{1} \oplus \boldsymbol{a}_k \quad (5)$$

where $\mathbf{1}$ represents an all-one vector of length L and $\oplus$ denotes the modulo-Q addition operation. After the processing of (5), each of the elements of $\boldsymbol{y}_k$ activates one from the Q frequencies based on the MFSK principles and this activated frequency is transmitted for one time-slot duration of T_h seconds. Specifically, the transmitted signal for the MFSK symbol X_k during $iT_s \leq t \leq (i+1)T_s$ can be expressed as

$$s_k(t) = \sum_{l=0}^{L-1} \sqrt{2P}\psi_{T_h}(t - iT_s - lT_h) \times \exp\left(2\pi[f_c + f_l^{(k)}]t + \varphi_l^{(k)}\right) \quad (6)$$

where P denotes the transmission power per dimension, $\psi_{T_h}(t)$ is the normalised pulse waveform of duration T_h, $f_l^{(k)}$ is the frequency tone determined by $a_k(l)$ and X_k, f_c is the carrier frequency, while $\varphi_l^{(k)}$ is the initial phase introduced by the MFSK and carrier modulations.

B. Receiver

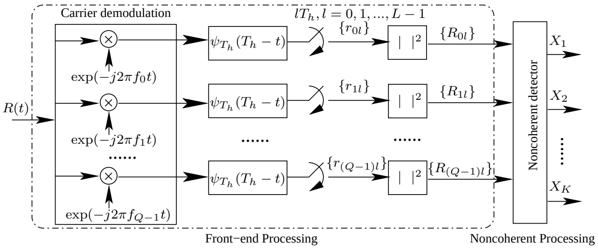

Fig. 3. Receiver schematic block diagram for the FFH/MFSK DMA system.

Let us assume that there are K CRUs communicating with a CR base-station (CRBS). The receiver schematic block diagram at the CRBS can be shown as Fig. 3. The receiver is divided into two sub-blocks: front-end processing and non-coherent processing. For simplicity, we assume synchronous FFH/MFSK DMA systems with ideal power-control. Consequently, the received complex low-pass equivalent signal at the CRBS can be expressed as

$$R(t) = \sum_{k=1}^{K} \sqrt{2P} \sum_{l=0}^{L-1} h_l^{(k)} \psi_{T_h}(t - lT_h) \exp(2\pi f_l^{(k)} t) + N(t)$$

where $h_l^{(k)}$ represents the channel gain corresponding to the frequency $f_l^{(k)}$ of the kth CRU and $N(t)$ is the complex valued additive white Gaussian noise (AWGN) process with zero mean and single-sided power spectral density (PSD) of N_0 per dimension. As shown in Fig. 3, the front-end processing sub-block is a typical noncoherent MFSK detector [14] excluding the decision-making device. It can be readily shown that, after some normalisation, the observation samples input to the noncoherent detector of Fig. 3 can be expressed as

$$\begin{aligned} R_{ml} =& |r_{ml}|^2 = |\sum_{k=1}^{K} h_m^{(k)} \delta[y_k(l), m] + n_{ml}|^2 \\ & m = 0, 1, ..., Q-1; \quad l = 0, 1, ..., L-1 \end{aligned} \tag{7}$$

where $\delta[x, y]$ is the Dirac delta function defined as $\delta[x, x] = 1$ and $\delta[x, y] = 0$ for $x \neq y$, n_{ml} is a complex Gaussian noise sample distributed with zero mean and a variance $\sigma^2 = LN_0/E_s$, where $E_s = PT_s$ denotes the energy per MFSK symbol.

In Fig. 3, the noncoherent detector can be either a single-user detector (SUD) or multiuser detector (MUD), which may be operated based either on soft-decision or on hard-decision observations [12]. Although they are capable of achieving better error performance, however, the noncoherent detectors based on soft-decision observations usually have significantly higher complexity than that based on hard-decision observations [13]. Hence, in this contribution, we focus on the noncoherent detectors operated based on hard-decision observations. Specifically, the error and throughput performance of the FFH/MFSK DMA systems employing MV-SUD or IIC-MUD [16] are investigated, when assuming communications over Nakagami-m fading channels. Let us now consider the MV-SUD and IIC-MUD in the next section.

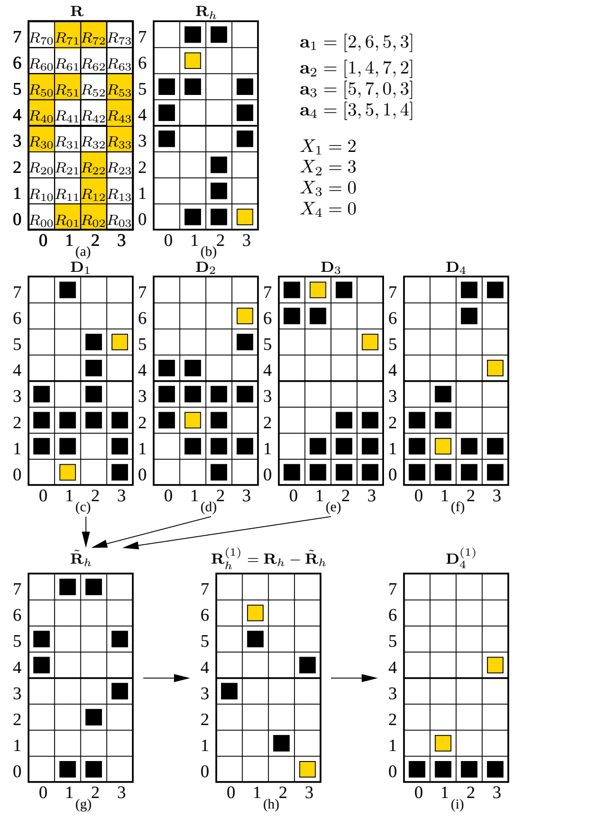

Fig. 4. TF matrices related to detection for $M = 4, Q = 8, L = 4$: (a) soft-decision observations; (b) hard-decision observations; (c), (d), (e) and (f) TF matrices formed after the frequency de-hopping of the TF matrix (b) using the FH addresses of CRU 1, 2, 3 and 4, respectively; (g) reference TF matrix formed by re-encoding the symbols detected for CRU 1, 2 and 3 using their corresponding FH addresses; (h) TF matrix after interference cancellation; (i) updated TF matrix for detection of CRU 4.

IV. Detection in FFH/MFSK DMA Systems

The MV-SUD and IIC-MUD considered start with constructing a $(Q \times L)$ time-frequency (TF) matrix $\boldsymbol{R} = [R_{ml}]$, as shown in Fig. 4 (a), using the decision variables $\{R_{ml}\}$ in (7), where Q and L correspond to the Q frequency tones and L time-slots per symbol duration, respectively. In Fig. 4 (a), the yellow entries are the elements activated by the four CRUs. In order to form the hard-decision TF observation matrix expressed by $\boldsymbol{R}_h$, let us assume that ν is a preset threshold. Then, whenever $R_{ml} \geq \nu$, the corresponding TF entry in $\boldsymbol{R}_h$ is marked or indicated by an element '1'. Otherwise, the (m, l)th entry of $\boldsymbol{R}_h$ is left empty or indicated by an element '0'. Correspondingly, the hard-decision TF matrix $\boldsymbol{R}_h$ is in the form of Fig. 4 (b), where the two yellow entries are the results of false-alarm.

In practical communications systems, however, it is usually very difficult to evaluate the optimal threshold for carrying out the hard-decision. For this sake, in this paper, an approach referred to as the expectation-based element selection (EES), which does not use threshold, is proposed for constructing the hard-decision TF observation matrix. In more detail, the EES approach is operated as follows. First, given K of the number of CRUs and Q of the available frequency bands, the expectation of the number of activated entries in $\boldsymbol{R}$ can be calculated, which is

$$E(\boldsymbol{R}) = L \times \sum_{i=1}^{\min(Q,K)} i \binom{Q}{i} f_{\boldsymbol{R}}(i) \tag{8}$$

when random FH addresses are assumed. In (8), $\binom{Q}{i} f_{\boldsymbol{R}}(i)$ is the probability of the event that i out of Q entries of a column in $\boldsymbol{R}$ are activated by the K CRUs, $f_{\boldsymbol{R}}(i)$ is the probability of the event that the given i entries of a column are activated by the K CRUs. Again, assuming random FH addresses, we can readily show that

$$f_{\boldsymbol{R}}(i) = \begin{cases} 1/Q^K, & i = 1 \\ \left(\dfrac{i}{Q}\right)^K - \displaystyle\sum_{j=1}^{i-1} \binom{i}{j} f_{\boldsymbol{R}}(i-1), & i \geq 2 \end{cases} \tag{9}$$

After knowing $E(\boldsymbol{R})$, then, the hard-decision TF observation matrix $\boldsymbol{R}_h$, as shown in Fig. 4(b), is formed from $\boldsymbol{R}$, as shown in Fig. 4(a), by marking a maximum $E(\boldsymbol{R})$ number of entries in $\boldsymbol{R}_h$, which correspond to the elements in $\boldsymbol{R}$ having the highest values. Furthermore, considering the fact that each column has at least one but no more than K elements activated, correspondingly, each column in $\boldsymbol{R}_h$ should have at least one but no more than K marked elements. Except the marked elements, all the other elements in $\boldsymbol{R}_h$ are empty. Now, the MV-SUD or IIC-MUD can be carried out based on $\boldsymbol{R}_h$, which is explained as the following steps enhanced by the example as shown in Fig. 4.

Step 1 - For both the MV-SUD and IIC-MUD, the TF matrix $\boldsymbol{R}_h$ is first de-hopped using the FH addresses $\boldsymbol{a}_1, \boldsymbol{a}_2, \ldots, \boldsymbol{a}_K$ of the K CRUs, forming the K detection matrices $\boldsymbol{D}_1, \boldsymbol{D}_2, \ldots, \boldsymbol{D}_K$, which are in the form of $\boldsymbol{D}_1, \boldsymbol{D}_2, \boldsymbol{D}_3$ and $\boldsymbol{D}_4$, as shown in Fig. 4(c), (d), (e) and (f), for the example considered.

Step 2 - Based on the detection matrices $\boldsymbol{D}_1, \boldsymbol{D}_2, \ldots, \boldsymbol{D}_K$, a decision is made for any of the CRUs, whose corresponding detection matrix contains only one majority row. Here the majority row is defined as the row with the maximum number of marked entries. The symbol value is decided as the index of the majority row. For example, as shown in Fig. 4, $\boldsymbol{D}_1, \boldsymbol{D}_2$ and $\boldsymbol{D}_3$ all have just one majority row. Hence, the symbols transmitted by CRU 1, 2 and 3 are detected as $\hat{X}_1 = 2$, $\hat{X}_2 = 3$ and $\hat{X}_3 = 0$. However, $\boldsymbol{D}_4$ has two majority rows. Therefore, for the IIC-MUD, the detection of CRU 4 is left to the following iterations. By contrast, when the MV-SUD is employed, the detection procedure completes at this step and decisions have to be made for those CRUs having more than one majority row. In this case, the symbol for a CRU can be detected as the index of a majority row chosen randomly from the majority rows.

Step 3 - At the ith iteration of the IIC-MUD, where $i = 1, 2, \ldots, i_{\max}$ with $i_{\max}$ representing the maximum number of iterations allowed, the following operations are executed. First, a reference matrix $\tilde{\boldsymbol{R}}_h$, as showed in Fig.4(g), is formed by re-encoding the symbols detected at the $(i-1)$th iteration using their corresponding FH addresses. Then, the TF observation matrix is modified from $\boldsymbol{R}_h^{(i-1)}$, where $\boldsymbol{R}_h^{(0)} = \boldsymbol{R}_h$, to $\boldsymbol{R}_h^{(i)}$ by deleting the entries in $\boldsymbol{R}_h^{(i-1)}$, which correspond to the marked entries in $\tilde{\boldsymbol{R}}_h$. For example, in Fig. 4, $\boldsymbol{R}_h^{(1)}$ is obtained from $\boldsymbol{R}_h^{(0)} = \boldsymbol{R}_h$ after applying the interference cancellation. Finally, based on the modified TF observation matrix $\boldsymbol{R}_h^{(i)}$, the detection is carried out for those CRUs having not been detected yet, in the same way as that of **Step** 2. For example, based on $\boldsymbol{R}_h^{(1)}$ of Fig. 4 (i), the detected symbol for the forth CRU is $\hat{X}_4 = 0$, which is now correctly detected.

Note that, for the IIC-MUD, the detection procedure completes either when all CRUs are detected, or when the maximum $i_{\max}$ number of iterations is reached, or when at a stage there are no detection matrices having only one majority row.

Note furthermore that, the IIC-MUD has a linear complexity, i.e., a complexity increasing linearly with the number of CRUs [16].

V. Performance Results

In this section, we provide some simulation results of the FFH/MFSK DMA systems using MV-SUD or IIC-MUD. In our simulations, we assumed that the arrival rate of PUs was $\lambda = 1$, the average time of a frequency band occupied by a PU was $1/\mu = 1/2$ and the number of frequency bands for the CR system was $Q = \bar{C}$. We assumed that each frequency band experienced independently identically distributed (iid) Nakagami-m fading [12], where the value of m characterises the severity of fading. Specifically, $m = 1$ and $1 < m < \infty$ correspond to Rayleigh and Rician fading channels, respectively, while $m \to \infty$ corresponds to Gaussian channels. For simulations of BER, it was assumed that $M \leq \bar{C} \leq C$. By contrast, for simulations of throughput, we assumed that $0 \leq \bar{C} \leq C$. Additionally, we assumed that CRUs used random FH addresses.

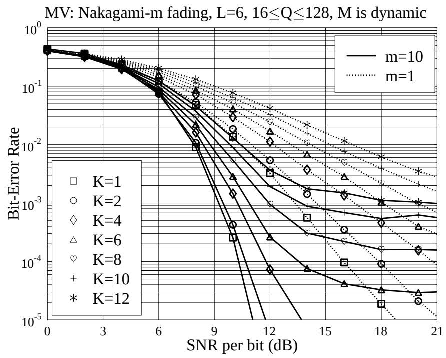

Fig. 5. BER versus average SNR per bit performance of the FFH/MFSK DMA systems employing MV-SUD, when communicating over Nakagami-m fading channels.

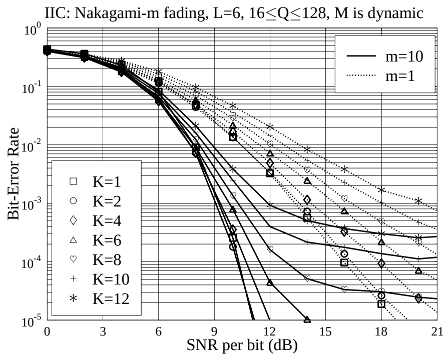

Fig. 6. BER versus average SNR per bit performance of the FFH/MFSK DMA systems employing IIC-MUD, when communicating over Nakagami-m fading channels.

Figs. 5 and 6 depict the BER performance of the FFH/MFSK DMA systems employing MV-SUD (Fig. 5) and IIC-MUD (Fig. 6), respectively, when communicating over Nakagami-m fading channels with the fading parameter $m = 1$ or 10. The parameters for the PRs were $C = 128, K_P = 8, C_P = 16$. In the CR systems, the value of M for MFSK was dynamic and set to $M = 2^{\text{int}(\log_2 \bar{C})}$, implying that the value of M is dependent on the value of $\bar{C}$. Additionally, for the IIC-MUD, $i_{\max} = K - 1$ was applied.

From the results of Figs. 5 and 6, we can be implied that the spectrum considered is capable of accommodating a substantial number of CRUs communicating based on the FFH/MFSK DMA, in addition to providing the required services for the PRs. As seen in Figs. 5 and 6, promising error performance may be attained at reasonable SNR values, owing to the merit that the FFH/MFSK DMA scheme can make efficient use of the frequency-diversity. Given the number of CRUs supported, the error performance improves as the channel quality improves. When comparing the results in Fig. 5 with that in Fig. 6, we can see that the IIC-MUD outperforms the MV-SUD. For examples, given $K = 6$, the FFH/MFSK DMA system using MV-SUD needs a SNR per bit of 18dB or 11dB to achieve a BER of 10^{-3}, when the fading parameter is $m = 1$ or $m = 10$. Correspondingly, given $K = 6$, the FFH/MFSK DMA system using IIC-MUD only needs a SNR per bit of about 15.5dB or 9.6dB to achieve the BER of 10^{-3}, when $m = 1$ or $m = 10$.

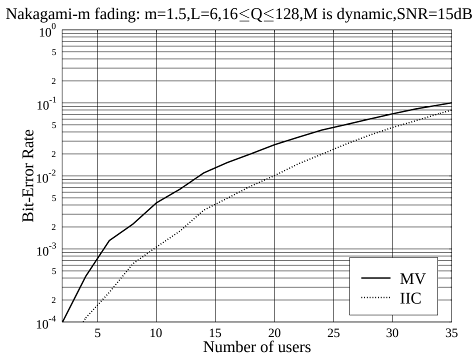

Fig. 7. BER versus number of CRUs of the FFH/MFSK DMA system employing MV-SUD and IIC-MUD, when the parameters for PRs are $C = 128, K_P = 8, C_P = 16$.

Fig. 7 illustrates the BER performance of the FFH/MFSK DMA systems employing the MV-SUD or IIC-MUD, when communicating over Nakagami-m fading channels associated with a fading parameter of $m = 1.5$. Again, the value of M was dynamic and was $M = 2^{\text{int}(\log_2 \bar{C})}$, and $i_{\max} = K-1$ was set for the IIC-MUD. Explicitly, the IIC-MUD outperforms the MV-SUD. For a required BER of 10^{-3}, the FFH/MFSK DMA system can support about 6 or 10 CRUs, when MV-SUD or IIC-MUD is invoked. By contrast, at a BER of 10^{-2}, the FFH/MFSK DMA system can support about 14 or 20 CRUs, when it employs MV-SUD or IIC-MUD.

Fig. 8 illustrates the throughput achievable by the FFH/MFSK DMA systems. The throughput depicted was evaluated as follows. Given the values of $Q = \bar{C}$ and M as well as the BER required, the maximum number of CRUs K can be determined. Then, the throughput is calculated as $K \times \log_2 M$. The results of Fig. 8 demonstrate that, with the aid of the FFH/MFSK DMA, a CR system is capable of attaining a substantial throughput, without affecting the communication quality of primary radio systems.

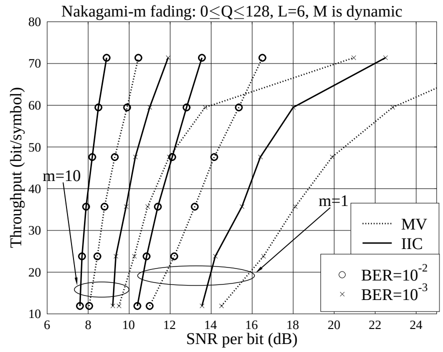

Fig. 8. Throughput achievable by the FFH/MFSK DMA system employing MV-SUD or IIC-MUD, when the parameters for PRs are $C = 128, K_P = 8, C_P = 16$.

In conclusion, we have proposed a FFH/MFSK DMA scheme for dynamically accessing the available frequency spectrums in CR environments. The studies demonstrate that a substantial throughput is attainable by the CRs. This throughput is achieved without QoS degradation of the PRs where the CR systems are embedded.

ACKNOWLEDGEMENT

The work of the first and third authors was supported by the National Basic Research Program of China (973 Program, Grant No. 2010CB731803).

REFERENCES

[1] FCC, *Spectrum Policy Task Force Report*, ET Docket No. 02-155, Nov. 2002.
[2] FCC. ET Docket No. 03-322. Notice of Proposed Rule Making and Order, Dec. 2003.
[3] J. Mitola, "Cognitive radio for flexible mobile multimedia communications," *Mobile Networks and Applications*, vol. 6, pp. 435 – 441, 2004.
[4] I. F. Akyildiz and et.al, "NeXt generation/dynamic spectrum access/cognitive radio wireless networks: A survey," *Computer Networks*, vol. 50, no. 13, pp. 2127 – 2159, 2006.
[5] T. Yucek and H. Arslan, "A survey of spectrum sensing algorithms for cognitive radio applications," *IEEE Comm. Surveys & Tutorials*, vol. 11, no. 1, pp. 116 – 130, 2009.
[6] I. F. Akyildiz and Y. Li, "OCRA: OFDM-based cognitive radio networks," *Broadband and Wireless Network Lab. Tech. Report*, Mar. 2006.
[7] T. Weiss, J. Hillenbrand, A. Krohn and F. K. Jondral, "Mutual interference in OFDM based spectrum pooling systems," *IEEE VTC2004*, vol. 4, pp. 1873 – 1877, May 2004.
[8] T. Weiss and F. Jondral, "Spectrum pooling: An innovative strategy for enhancement of spectrum efficiency," *IEEE Comm. Mag.*, vol. 42, no. 3, pp. 8 – 14, Mar. 2004.
[9] D. Kendall, "Stochastic processes occurring in the theory of queues and their analysis by the method of the imbedded Markov chain," *The Annals of Math. Statistics*, vol. 24, no. 3, pp. 338 – 354, 1953.
[10] A. Goldsmith and et.al, "Breaking spectrum gridlock with cognitive radios: an information theoretic perspective," *Proceedings of the IEEE*, vol. 97, no. 5, pp. 894 – 914, May 2009.
[11] D. Bertsekas and R. Gallager, *Data Networks* (2nd Ed.). Prentice Hall, Upper Saddle River, New Jersey, USA, 1992.
[12] L.-L. Yang, *Multicarrier Communications*. Chichester, United Kingdom: John Wiley, 2009.
[13] S. Zhang, L.-L. Yang and Y. Zhang, "Dynamic FFH/MFSK for multiple-access in cognitive radios," *ISWCS'2010*, York, UK, Sept. 2010.
[14] J. G. Proakis, *Digital Communications* (3rd Ed.). McGraw Hill, 1995.
[15] T. Mabuchi, R. Kohno and H. Imai, "Multiuser detection scheme based on canceling cochannel interference for MFSK/FH-SSMA system," *IEEE J. on Select. Areas in Comm.*, vol. 12, no. 4, pp. 593 – 604, May 1994.
[16] U. Fiebig, "Iterative interference cancellation for FFH/MFSK MA systems," *IEE Proc. Comm.*, vol. 143, pp. 380 – 388, Dec. 1996.
[17] K. W. Halford and M. Brandt-Pearce, "Multistage multiuser detection for FHMA," *IEEE Trans. on Comm.*, vol. 48, no. 9, pp. 1550 – 1562, Sept. 2000.